Radiation Dosimetry of ^{99m}Tc-PSMA I&S: A Single-Center Prospective Study

Szabolcs Urbán[1], Catherine Meyer[2,3], Magnus Dahlbom[2,3], István Farkas[1], Gábor Sipka[1], Zsuzsanna Besenyi[1], Johannes Czernin[2,4,5], Jeremie Calais[*2–5], and László Pávics[*1]

[1]*Department of Nuclear Medicine, University of Szeged, Szeged, Hungary;* [2]*Ahmanson Translational Theranostics Division, Department of Molecular and Medical Pharmacology, University of California Los Angeles, Los Angeles, California;* [3]*Physics & Biology in Medicine Interdepartmental Graduate Program, David Geffen School of Medicine, University of California Los Angeles, Los Angeles, California;* [4]*Jonsson Comprehensive Cancer Center, University of California Los Angeles, Los Angeles, California; and* [5]*Institute of Urologic Oncology, University of California Los Angeles, Los Angeles, Los Angeles, California*

^{99m}Tc-PSMA I&S is a prostate-specific membrane antigen (PSMA) tracer that can be used for planar and SPECT/CT γ-imaging and radioguided surgery. The primary aim of this study was to estimate the dosimetry of ^{99m}Tc-PSMA I&S using a hybrid method (sequential γ-planar imaging and 1 single SPECT/CT) in healthy volunteers. The secondary aim was to depict the tracer biodistribution and tumor-to-background ratios (TBRs) in patients with prostate cancer (PCa). **Methods:** Dosimetry of ^{99m}Tc-PSMA I&S was investigated in 4 healthy volunteers. Whole-body planar imaging was acquired at 1, 2, 3, 6, and 24 h and SPECT/CT at 6 h after tracer injection. Contours of organs were drawn on all acquisitions to determine organ activity at each time point. Absorbed dose was estimated using 2 methods: independent curve-fitting manual method (Levenberg-Marquardt–based algorithm using dose factors from RAdiation Dose Assessment Resource [RADAR] website) and OLINDA/EXM software (version 2.0; HERMES Medical Solutions). Biodistribution of ^{99m}Tc-PSMA I&S was assessed in 10 patients with PCa on SPECT/CT images at 6 h. Tumor uptake (SUV_{max}), and TBR (tumor SUV_{max}/background organ SUV_{mean}) using muscle (T/M), bladder (T/B), and intestine (T/I) as background organs were determined. **Results:** The mean injected activity of ^{99m}Tc-PSMA I&S was 717 MBq (range: 562–828 MBq). No adverse events related to the injection of ^{99m}Tc-PSMA I&S were reported. The average radiation effective dose was 0.0055 mSv/MBq with the RADAR manual method and 0.0052 mSv/MBq with OLINDA/EXM. Total body effective dose ranged between 3.33–4.42 and 3.11–4.23 mSv, respectively. All PCa patients showed high tracer uptake in primary and metastatic lesions with T/M, T/B, and T/I ranging from 5.29–110, 0.11–7.02, and 0.96–16.30, respectively. **Conclusion:** Effective doses of ^{99m}Tc-PSMA I&S were comparable to those known for most of the ^{99m}Tc tracers and was lower than for the ^{68}Ga-labeled and ^{18}F-labeled agents. ^{99m}Tc-PSMA I&S SPECT/CT showed high TBR in PCa patients. This study can provide required data for translation and approval of ^{99m}Tc-PSMA I&S by regulatory agencies.

Key Words: dosimetry; 99mTc-Mas3-y-nal-k(Sub-KuE); PSMA I&S; prostate cancer; SPECT/CT

J Nucl Med 2021; 62:1075–1081
DOI: 10.2967/jnumed.120.253476

Received Jul. 15, 2020; revision accepted Nov. 16, 2020.
For correspondence or reprints, contact Szabolcs Urbán (urban.szabolcs@med.u-szeged.hu).
Published online December 4, 2020.

Prostate-specific membrane antigen (PSMA) is a transmembrane metallopeptidase protein highly overexpressed on the surface of prostate cancer (PCa) cells, thus representing a relevant target for PCa nuclear theranostics (*1*). In the past decade, thousands of PSMA PET scans have been obtained worldwide for staging and restaging PCa, reflecting the rapid and profound clinical adoption by the urooncologist community. ^{99m}Tc is the most widely used radionuclide for diagnostic imaging; therefore, ^{99m}Tc-labeled PSMA compounds could be a valuable cost-effective alternative in regions in which access to PSMA PET imaging is limited. ^{99m}Tc-PSMA imaging can also enable radioguided surgery (RGS) with intraoperative γ-detection. PSMA-targeted RGS can help and guide urologists to detect PCa lymph node (LN) metastasis during surgery. Different ^{99m}Tc-PSMA compounds have been developed. ^{99m}Tc-Mas3-y-nal-k(Sub-KuE) (^{99m}Tc PSMA I&S) is a nonpatented compound derived from the PSMA I&T precursor that can be obtained with a reliable kit-labeling procedure (*2*). Previous work has shown the utility of ^{99m}Tc-PSMA I&S for RGS in large retrospective cohorts with improved treatment outcome (*3,4*). As a required step for further translation and approval by regulatory agencies, the primary objective of this study was to provide the radiation dosimetry analysis of ^{99m}Tc-PSMA I&S in healthy volunteers using a hybrid imaging method (sequential γ-planar imaging and a single SPECT/CT). The secondary aim was to describe the biodistribution of ^{99m}Tc-PSMA I&S in PCa patients at 6 h after tracer injection.

MATERIALS AND METHODS

Study Design and Patients

This is a prospective study of radiation dosimetry and biodistribution of a novel ^{99m}Tc-PSMA imaging probe. The study protocol was approved by the local institutional ethics committee for human biomedical trials at the University of Szeged (license no. 229/2017-SZTE, date of approval November 20, 2017). The imaging data were acquired at the University of Szeged, in Hungary. Four healthy men clinically free from any malignant disease were enrolled in the dosimetry study. Ten patients with newly diagnosed PCa were enrolled in the biodistribution study. All patients provided oral and written consent after receiving detailed information of the study and agreed to the collection of data. The analysis was conducted at the University of Szeged in Hungary and at the University of California in Los Angeles, California (material transfer agreement MTA2020-00000538).

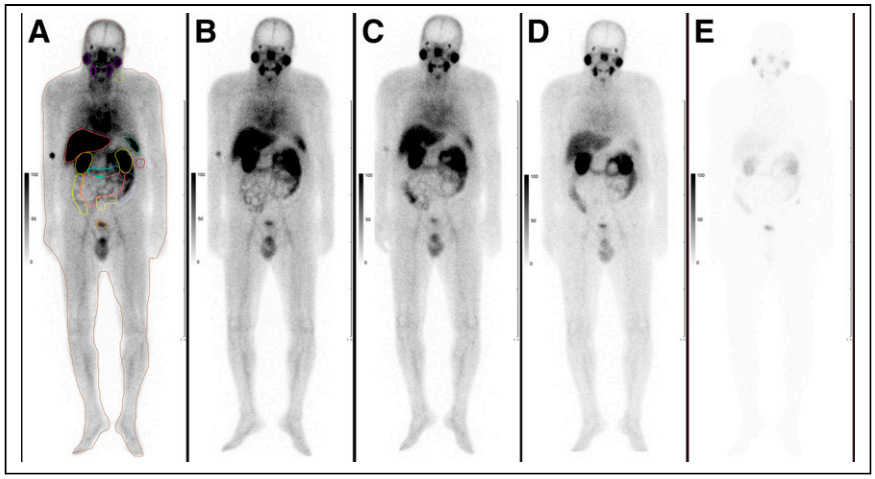

FIGURE 1. Example of source organs and background ROIs in a healthy volunteer (patient 003) on planar scintigraphy images (A); WB anterior and posterior ^{99m}Tc-Mas3-y-nal-k(Sub-KuE) scintigraphy was performed at 1, 2, 3, 6, and 24 h after injection (A–E).

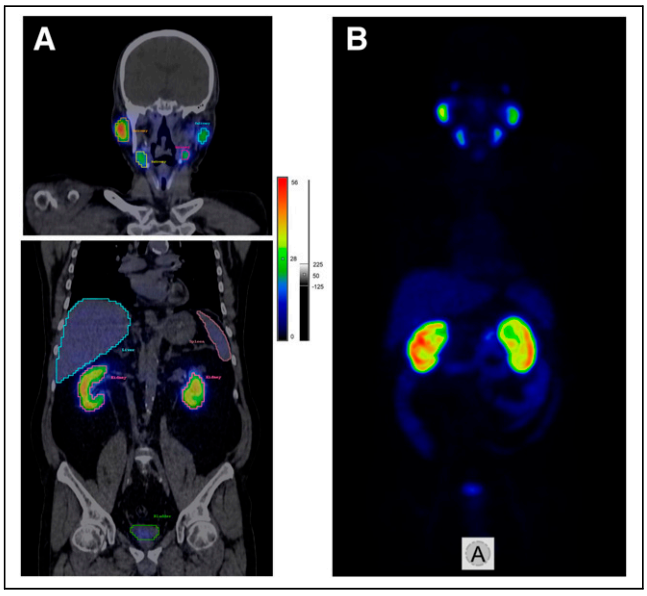

FIGURE 2. (A) Example of organ delineation in healthy/PCa patient (patient 003) on SPECT/CT images. (B) ^{99m}Tc-PSMA I&S SPECT 3-dimesional maximum-intensity projection.

Synthesis and Quality Control of ^{99m}Tc-PSMA I&S

Synthesis of Mas3-y-nal-k(Sub-KuE) peptide-lyophilisate has been previously reported (*2*). ^{99m}Tc-pertechnetate was obtained from a ^{99}Mo/^{99m}Tc generator. A single-dose freeze-dried kit contains 25 μg of peptide. Radiolabeling was performed with 5.87–7.53 GBq of ^{99m}Tc-pertechnetate. Radiochemical purity analysis was performed by instant thin-layer chromatography medium paper impregnated with a silica gel. As a solvent, we used methyl ethyl ketone. Radiochemical purities were in all cases greater than 95%.

Image Acquisition

A hybrid imaging method was used to determine the dosimetry of ^{99m}Tc-PSMA I&S: multiple-time-point whole-body (WB) planar imaging and a single quantitative SPECT/CT scan. In all healthy subjects (n = 4), WB anterior and posterior scintigraphy was performed at 1, 2, 3, 6, and 24 h after radiopharmaceutical administration (Fig. 1) using a triple-head γ-camera (AnyScan Trio SPECT/CT; Mediso Medical Imaging Systems Ltd.), equipped with low-energy, high-resolution collimators. The scanning speed was 18 cm/min, a matrix size of 256 × 1,024 pixels was used, and a symmetric 20% window was set at 140 keV. In all volunteers and PCa patients (n = 14), WB (mid thighs to vertex) SPECT/CT images were acquired at 6 h after radiopharmaceutical administration (Fig. 2). Quantitative SPECT images were acquired using a 128 × 128 matrix with a 20% energy window centered at 140 keV with adjacent scatter correction windows. A total of 96 projection views were acquired over 360° in 3.75° steps at 10 s per view. The number of bed positions was 3. Reconstruction of raw SPECT data was performed using the iterative Tera-Tomo (Mediso Medical Imaging Systems Ltd.) software, which is based on the order of sets and subsets (48 iterations/4 subsets) method. CT-based attenuation correction and point spread function correction were used. CT images were acquired using low-dose CT (120 keV, 100 mAs, 1.5 pitch factor, and 2.5 mm slice thickness). To improve the visibility of the gastrointestinal tract, Macrogol 1500 (50 g/L) (Molar Chemicals Ltd.) was administered orally 1 h before SPECT/CT imaging.

Determination of Absorbed Doses

The source organs consisted of the salivary glands, kidneys, liver, small intestine, large intestine, spleen, urinary bladder, and the body remainder. Source organ contours and appropriate background regions of interest (ROIs) were delineated manually on the anterior and posterior WB images at 1 h after injection (Fig. 1). All ROIs were manually relocated on the subsequent images and were validated by 2 experienced nuclear medicine physicians.

The mean counts were obtained for each organ and background ROI. Background-corrected organ counts were then calculated (based on the number of pixels from the organ ROI) for both anterior and posterior WB images. The geometric mean count was determined for every organ from the background-corrected anterior and posterior counts.

Source organ volumetric contours were delineated manually on CT images. The volumes of interest (VOIs) were transferred to the registered quantitative SPECT scans to determine the activity inside the source organs at 6 h after injection (Fig. 2). The fraction of injected activities were determined at each time point using the geometric mean counts from the planar images and the activity from the SPECT images.

The time–activity-curves were fitted with a mono- or biexponential function using the Levenberg-Marquardt–based algorithm and were generated for every source organ.

Absorbed doses for the target organs were estimated based on the RAdiation Dose Assessment Resource (RADAR, www.doseinfo-radar.com) scheme using the equation $D_T = \sum_S N_S \times DF(D \leftarrow S)$, where D_T is the dose of a given target organ, N_S is the number of disintegrations that occur in a source organ, and DF is the dose factor, which gives the absorbed dose in a target per disintegration in a source (*5*). Integration of the time–activity curve was calculated for every source organ. Patient-specific volumes were used for the liver, kidneys, small intestines, spleen, salivary glands, and body remainder mass determination.

TABLE 1
Patients Characteristics

Patient	Age (y)	Weight (kg)	Indication	PSA (ng/mL)	Gleason score	Injected activity (MBq)
001	57	95	Healthy volunteer	NA	NA	674
002	68	92	Healthy volunteer	NA	NA	804
003	64	83	Healthy volunteer	NA	NA	828
004	70	84	Healthy volunteer	NA	NA	562
005	64	81	Initial staging of PCa	8.84	6	634
006	66	110	Initial staging of PCa	11.37	7	553
007	67	86	Initial staging of PCa	1.02	10	682
008	73	120	Initial staging of PCa	0.34	7	748
009	63	130	Initial staging of PCa	21.2	7	698
010	70	85	Initial staging of PCa	18.46	8	692
011	66	78	Initial staging of PCa	4.23	9	780
012	74	90	Initial staging of PCa	4.21	7	821
013	71	54	Initial staging of PCa	44.3	7	714
014	64	110	Initial staging of PCa	18.2	10	624

In a second step, the curve-fitting and dose calculations were performed using OLINDA/EXM software (version 2.0; Hermes Medical Solutions), for comparison and method validation. For each volunteer, the non–decay-corrected percentage injected activity in the source organs at each time point was used to generate time–activity curves. The same patient-specific volumes were used as in the manual method. Biexponential curve-fitting in OLINDA/EXM version 2.0 was used to fit the time–activity curves. The individual volunteer dose reports were compiled as mean ± SD. Effective dose calculations were done using tissue-weighting factors according to recommendations of the International Commission on Radiological Protection (*6*).

Biodistribution in PCa Patients

The PROMISE miTNM scoring system was used to report the scan findings (*7*). Tumor, bladder, and intestine volumetric contours were manually delineated on the SPECT/CT images (+6 h) by 2 experienced nuclear medicine physicians. A background VOI with the same size as the tumor VOI was placed on gluteal muscles to quantify muscle background uptake. Using patient weight, injected activity, and ^{99m}Tc camera calibration factor, we calculated the SUVs as follows: SUV_{mean} (g/mL) = (total radioactivity/volume of VOI)/(injected radioactivity/body weight) and SUV_{max} (g/mL) = (maximum radioactivity/volume of VOI)/(injected radioactivity/body weight). TBRs were calculated as follows: tumor/muscle (T/M, tumor SUV_{max}/muscle SUV_{mean}), tumor/bladder (T/B, tumor SUV_{max}/bladder SUV_{mean}), and tumor/intestine (T/I, tumor SUV_{max}/intestine SUV_{mean}) ratios.

Statistics

Descriptive statistics were used (median, mean, range). The Wilcoxon signed-rank test was used to compare the doses obtained with the 2 methods.

RESULTS

Patients

Patients were enrolled from December 14, 2017, to November 14, 2018. In the dosimetry cohort of healthy volunteer men (n = 4), the median age was 66 y (range: 57–70 y), and the median weight was 88 kg (range: 83–95 kg) (Table 1). In the biodistribution cohort of patients with newly diagnosed PCa (n = 10), the median age was 67 y (range: 63–74 y), and the median weight was 88 kg (range: 54–130 kg) (Table 1). The median prostate-specific antigen (PSA) was 10.1 ng/mL (range: 0.34–44.3 ng/mL). The number of patients with a PCa disease Gleason score of 6, 7, 8, 9, and 10 was 1 (10%), 5(50%), 1 (10%), 1 (10%), and 2 (20%), respectively.

Radiation Dosimetry in Healthy Volunteers

The median injected activity of ^{99m}Tc-PSMA I&S was 739 MBq (range: 562–828 MBq). No adverse events related to the injection of ^{99m}Tc-PSMA I&S were reported. ^{99m}Tc-PSMA I&S uptake was observed mainly in the salivary glands, liver, kidneys, spleen, small intestine, large intestine, and urinary bladder. Figure 3 depicts an example of time–activity curves of normal organs in a healthy volunteer (patient 003). Absorbed and effective doses using the manual RADAR and OLINDA/EXM methods are presented in Table 2. Detailed fitting parameters are presented in Supplemental Table 1 (supplemental materials are available at http://jnm.snmjournals.org).

When the OLINDA/EXM method was used, the mean absorbed dose (mGy/MBq) was the highest in the kidneys (0.0733 mGy/MBq) followed by the salivary glands (0.0221 mGy/MBq), the adrenals (0.0217 mGy/MBq), the liver (0.0123 mGy/MBq), the spleen (0.0119 mGy/MBq), and the small intestine (0.0119 mGy/MBq). Total-body effective doses of the 4 volunteers were: 0.0053 (patient 001), 0.0048 (patient 002), 0.0051 (patient 003), and 0.0055 (patient 004) mSv/MBq. The average total-body effective dose was 0.0052 mSv/MBq. When the injected activities (range: 562–828 MBq) were considered, the effective doses of the 4 volunteers were between 3.11 and 4.23 mSv.

When the manual RADAR method was used, the effective doses of the 4 volunteers were: 0.0052 (patient 001), 0.0056 (patient 002), 0.0053 (patient 003), and 0.0059 (patient 004) mSv/MBq, with an average effective dose of 0.0055 mSv/MBq. When the injected activities (range: 562–828 MBq) were considered, the effective doses of the 4 volunteers were between 3.33 and 4.42

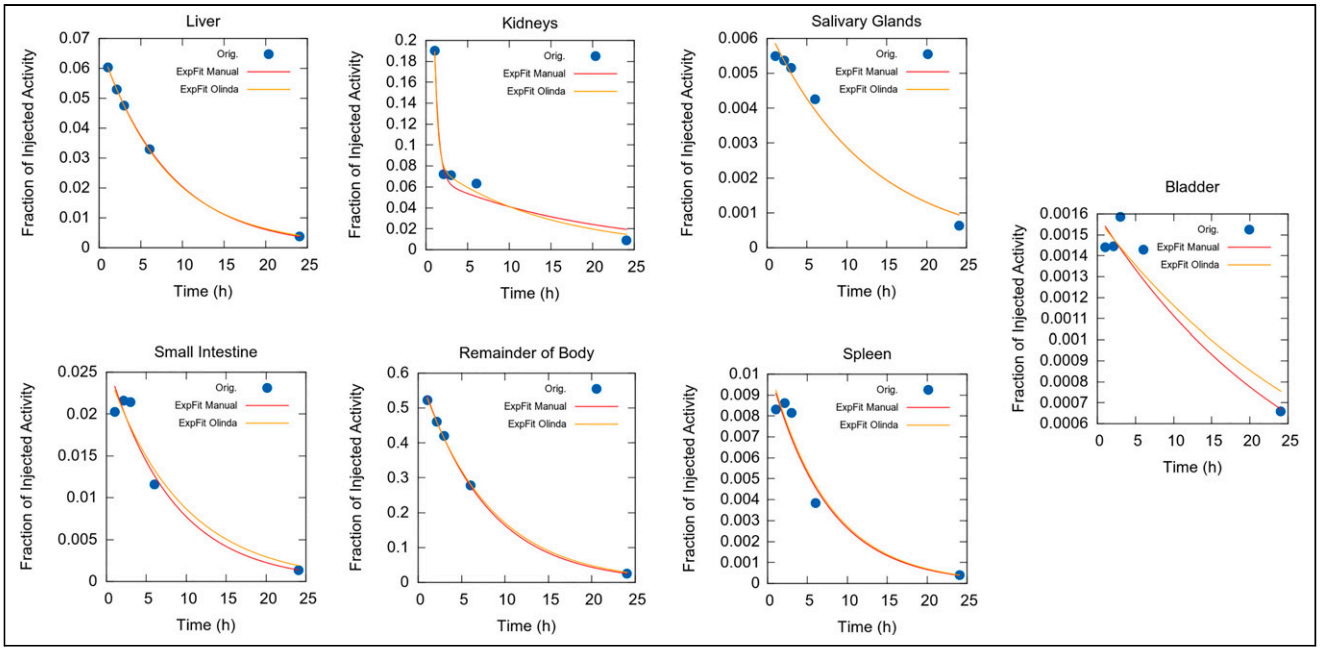

FIGURE 3. Time–activity curves of normal organs in a healthy volunteer (patient 003).

mSv. Between methods, the dose values were very similar; the largest difference observed in mean effective dose was for the liver (9.5% difference), except gastrointestinal tract, which was defined differently in the 2 methods. There was no statistically significant difference between the paired mean effective doses (mSv/MBq) obtained by the 2 methods (paired Wilcoxon signed-rank test, $P > 0.05$, lower large intestine/upper large intestine and left/right colon were excluded).

Biodistribution Study in Patients with Prostate Cancer

The median injected activity of ^{99m}Tc PSMA I&S was 695 MBq (range: 553–821 MBq). No adverse events related to the injection of ^{99m}Tc-PSMA I&S were reported. High uptake of ^{99m}Tc-PSMA I&S was observed 6 h after injection both in primary tumors (10/10 patients [100%], mean SUV_{max}: 13.37 [range: 3.25–44.00]), and in metastatic lesions (3/10 patients [30%], mean SUV_{max}: 5.71 [range: 1.80–8.48]) (Table 3). The mean T/M ratio, T/B ratio, and T/I ratio in the primary tumors was 30.22 (range: 7.95–110.00), 1.59 (range: 0.11–7.02), and 5.56 (range: 0.96–16.30), respectively, and in the metastasis 14.97 (range: 5.29–24.23), 0.60 (range: 0.33–0.92), and 3.16 (range: 1.20–4.82), respectively. Figure 4 shows pathologic tracer uptake in primary PCa (patient 012) and in patients with metastases in bone (patient 011) and LNs (patient 014). On the basis of the SPECT counts, the average activity of the pathologic lesions 6 h after tracer injection was 0.16 MBq (range: 0.01–0.96 MBq). On the basis of the physical half-life of ^{99m}Tc, the average lesion activity after 24 and 48 h was estimated to be 19.73 kBq (range: 1.25–120.00 kBq) and 1.23 kBq (range: 0.08–7.55 kBq), respectively.

DISCUSSION

Herein we report the radiation dose deposition of ^{99m}Tc-PSMA I&S in organs of 4 healthy volunteer patients with a hybrid imaging method (multiple sequential time-point planar imaging and a single SPECT/CT). Radiation dosimetry analysis is required for further clinical translation and approval by regulatory agencies. The average effective whole-body dose for administration of 700 MBq of ^{99m}Tc-PSMA I&S was 3.63 ± 0.64 mSv (OLINDA/EXM). The mean effective dose of ^{99m}Tc-PSMA I&S (0.0052 mSv/MBq) is similar to conventional ^{99m}Tc- MDP (*8*) used in SPECT/CT scans (0.004 mSv/MBq).

Several other ^{99m}Tc-PSMA compounds have been developed including, among others, Tc-EDDA/HYNIC-iPSMA (*9*), ^{99m}Tc-tricarbonyl-iPSMA (*10*), ^{99m}Tc-MIP-1404, and ^{99m}Tc-MIP-1405 (*11*). In comparison with currently available Tc-labeled PSMA inhibitors, the effective dose of ^{99m}Tc-PSMA I&S (0.0052 mSv/MBq) is similar to ^{99m}Tc-EDDA/HYNIC-iPSMA (0.0046 mSv/MBq) and lower than ^{99m}Tc-MIP-1404 (0.0088 mSv/MBq) and ^{99m}Tc-MIP-1405 (0.0079 mSv/MBq) agents. The radiation-absorbed dose of 740 MBq of ^{99m}Tc PSMA I&S in the liver (9.10 mSv) was lower than that of ^{99m}Tc-EDDA/HYNIC-iPSMA (liver = 10.73 mSv); however, the small intestine (8.83 mSv), spleen (8.83 mSv), kidneys (54.24 mSv), and salivary glands (16.35 mSv) had higher doses than ^{99m}Tc-EDDA/HYNIC-iPSMA (small intestine = 2.42 mSv, spleen = 7.06 mSv, kidney = 28.80 mSv, salivary glands = 9.69 mSv) (*9*). In comparison to the PET tracers, the effective dose of ^{99m}Tc-PSMA I&S is lower than ^{68}Ga-labeled (^{68}Ga-PSMA-11 (0.0236 mSv/MBq (*12*)) and ^{18}F-labeled (0.0220 mSv/MBq (*13*)) PSMA-targeted tracers.

The dose calculation and verification using OLINDA/EXM (version 2.0) software contained the same main steps. The largest difference was in the exponential curve-fitting method: OLINDA was used for biexponential curve fitting in every case, whereas the manual method used mono- or biexponential fitting, based on visual assessment. As shown in Figure 3, there were cases when the monoexponential fit was adequate (liver, spleen, remainder of body by visual inspection). Therefore, there were only minor differences in the calculated number of disintegrations of source organs between both methods. Another difference was the segment definition of the gastrointestinal tract:

TABLE 2
Organ Absorbed and Effective Doses of ^{99m}Tc-Mas3-Y-nal-k(Sub-KuE) Using Manual RADAR and OLINDA/EXM 2.0 Methods

	Manual RADAR			OLINDA/EXM		
	Organ doses (mGy/MBq)		Mean effective doses (mSv/MBq)	Organ doses (mGy/MBq)		Mean effective doses (mSv/MBq)
Target organ	Mean	SD		Mean	SD	
Adrenals	2.17E–02	4.54E–03	2.00E–04	2.17E–02	5.62E–03	2.00E–04
Brain	2.13E–03	1.59E–04	2.13E–05	2.15E–03	2.20E–04	2.15E–05
Esophagus	4.08E–03	2.60E–04	1.63E–04	3.98E–03	3.12E–04	1.59E–04
Eyes	2.02E–03	1.69E–04	0.00E–00	2.04E–03	2.23E–04	0.00E+00
Gallbladder wall	8.98E–03	6.34E–04	8.30E–05	8.22E–03	5.89E–04	7.59E–05
LLI/left colon	1.02E–02	1.74E–03	4.94E–04	8.90E–03	7.57E–04	4.31E–04
Small intestine	1.15E–02	3.93E–03	1.07E–04	1.19E–02	3.82E–03	1.10E–04
Stomach wall	5.11E–03	2.84E–04	6.13E–04	5.00E–03	4.03E–04	6.00E–04
ULI/right colon	1.12E–02	2.66E–03	5.43E–04	8.49E–03	1.03E–03	4.12E–04
Rectum	4.56E–03	7.54E–04	1.05E–04	4.45E–03	4.74E–04	1.02E–04
Heart wall	4.12E–03	2.65E–04	3.80E–05	4.00E–03	3.01E–04	3.69E–05
Kidneys	7.20E–02	2.34E–02	6.64E–04	7.33E–02	2.66E–02	6.77E–04
Liver	1.35E–02	1.92E–03	5.43E–04	1.23E–02	1.76E–03	4.93E–04
Lungs	3.46E–03	2.36E–04	4.15E–04	3.37E–03	2.82E–04	4.05E–04
Pancreas	7.59E–03	4.58E–04	7.01E–05	7.23E–03	2.77E–04	6.67E–05
Prostate	4.60E–03	6.36E–04	2.12E–05	4.50E–03	3.74E–04	2.08E–05
Salivary glands	2.32E–02	3.05E–03	2.32E–04	2.21E–02	3.02E–03	2.21E–04
Red marrow	3.43E–03	1.79E–04	4.12E–04	3.41E–03	2.56E–04	4.10E–04
Osteogenic cells	6.39E–03	3.80E–04	6.39E–05	6.45E–03	5.03E–04	6.45E–05
Spleen	1.23E–02	3.31E–03	1.14E–04	1.19E–02	3.07E–03	1.10E–04
Testes	2.24E–03	1.66E–04	8.94E–05	2.25E–03	1.97E–04	9.00E–05
Thymus	2.79E–03	2.21E–04	2.58E–05	2.78E–03	2.77E–04	2.57E–05
Thyroid	2.59E–03	2.11E–04	1.03E–04	2.62E–03	2.68E–04	1.05E–04
Urinary bladder wall	9.54E–03	6.18E–03	3.81E–04	8.89E–03	4.92E–03	3.55E–04
Total body	3.03E–03	2.54E–04	0.00E–00	3.15E–03	3.08E–04	0.00E+00

LLI = lower large intestine; ULI = upper large intestine.

RADAR contains dose factors for the upper large intestine and lower large intestine, whereas OLINDA/EXM calculates doses to the left and right colon.

Detailed biodistribution data for ^{99m}Tc-PSMA I&S has been published by Robu et al. (*2*). Relatively high blood and background activity were observed due to the high plasma protein binding of the radiopharmaceutical (94%). ^{99m}Tc-PSMA I&S is excreted primarily by the urinary system, although increased lipophilicity of the tracer enhanced liver uptake and produced a higher constant rate of hepatobiliary clearance, which led to increased intestinal activity. In our study, intestinal tracer accumulation was found to be highly variable as well as bladder activity.

Both SPECT/CT imaging systems and SPECT tracers are more affordable than PET/CT systems. ^{99m}Tc-PSMA I&S can represent a valuable alternative to PSMA PET imaging in countries in development. Another potential application of ^{99m}Tc-PSMA I&S is RGS. PSMA-targeted RGS can help guide urologists to detect PCa LN metastasis during surgery. PSMA-expressing LNs can be detected intraoperatively using a γ-probe. Despite the use of PSMA-targeted PET as a tool for preoperative guidance, intraoperative detection and resection of small lesions remains challenging, especially because of the small dimension of the LN metastasis, the technical difficulty of pelvic LN dissection, and atypical anatomic localization of the LNs. Farolfi et al. reported that in up to two thirds of patients who experienced disease recurrence after surgery, at least 1 lesion had already been detected on the preoperative PSMA-targeted PET imaging, suggesting that LN dissection was often not complete (*14*). PSMA-targeted RGS might increase a surgeon's confidence in intraoperative detection and complete dissection of metastatic LNs lesions detected in the preoperative PSMA-targeted SPECT and PET imaging. European retrospective studies conducted in large cohorts reported high rates of

TABLE 3
Biodistribution Study of ^{99m}Tc-PSMA I&S in Patients with PCa

Patient	Gleason score	PSA (ng/mL)	PROMISE miTNM	Tumor SUV_{max}		T/M ratio		T/B ratio		T/I ratio	
				PCa	Metastasis	PCa	Metastasis	PCa	Metastasis	PCa	Metastasis
005	6	8.84	miT2uN0M0	10.95		19.55		0.12		1.25	
006	7	11.37	miT2mN0M0	5.09		7.95		0.28		2.81	
007	10	1.02	miT2uN0M0	8.1		11.57		0.94		1.6	
008	7	0.34	miT2uN0M0	5.18		8.09		0.14		2.3	
009	7	21.2	miT2uN0M0	44		110		7.02		16.3	
010	8	18.46	miT3bN0M1b(oligo)	16	1.8	47.06	5.29	4.15	0.47	10.67	1.20
011	9	4.23	miT2uN0M1b(oligo)	11.89	4.25;7.67	25.85	9.24;16.67	0.92	0.33;0.60	6.1	2.18;3.93
012	7	4.21	miT2uN0M0	22		42.3		1.42		9.44	
013	7	44.3	miT2uN0M0	3.25		9.03		0.11		0.96	
014	10	18.2	miT4N2b(RP,CIR,OBR)M0	7.29	3.82;8.23;8.48	20.83	10.91;23.51;24.23	0.79	0.42;0.89;0.92	4.14	2.17;4.68;4.82

T/M = tumor-to-muscle background ratio; T/B = tumor-to- bladder background ratio; T/I = tumor-to-intestine background ratio.

FIGURE 4. Low-dose CT (A) and ^{99m}Tc-PSMA SPECT/CT (B) images of a PCa primary tumor lesion (patient 012) with high TBR (SUV_{max}: 22.00, TBR: 42.30 [arrowheads]). Low-dose CT (C) and ^{99m}Tc-PSMA SPECT/CT (D) images of a PCa bone metastasis (patient 011) with high TBR (SUV_{max}: 11.89, TBR: 25.85 [arrowheads]). Low-dose CT (E) and ^{99m}Tc-PSMA SPECT/CT (F) images of PCa LN metastases (patient 014) with high TBR (SUV_{max}: 8.23, TBR: 23.51 and SUV_{max}: 8.48, TBR: 24.23 [arrowheads]).

intraoperative tumor detection validated by histopathology, as well as improved treatment outcome (*3,4*). Of note, a first European clinical trial is currently investigating the feasibility of PSMA-targeted RGS (TRACE: NCT03857113).

The timing of tracer administration for RGS has been determined empirically and may be improved. In this cohort, the activity in the target lesions of between 24 and 48 h after injection remains in the detectable range for commercially available γ-probes. The minimum acceptable sensitivity of a γ-probe system sensitivity for clinical use is 2.5 cps/kBq (*15*). Therefore, the γ-probe could detect the tumors between 24 and 48 h after tracer administration. Even though ^{99m}Tc-PSMA I&S showed good TBR in both primary and metastatic lesions, differentiation between pathologic and physiologic uptake can be difficult because of the urinary and intestinal tracer accumulation. On the basis of our TBRs, tumor differentiation from the intestine seems to be easier than from the bladder on the SPECT/CT at more than 6 h. However, after 24 h, a lower activity is expected due to urinary and intestinal elimination in contrast with the stable tumor uptake.

CONCLUSION

This dosimetry study of ^{99m}Tc-PSMA I&S showed that injected activities of 562–828 MBq translate to estimated effective doses of 3.33–4.42 mSv (manual RADAR method) and 3.11–4.23 mSv (OLINDA/EXM method), which is similar to the effective doses from other ^{99m}Tc-PSMA inhibitors. Preliminary data suggest high TBR of primary and metastatic PCa lesions. Larger trials are needed to further define its capabilities in the management of PCa.

DISCLOSURE

No potential conflict of interest relevant to this article was reported.

KEY POINTS

QUESTION: What is the radiation dosimetry and biodistribution of ^{99m}Tc-PSMA I&S?

PERTINENT FINDINGS: On the basis of a hybrid method using serial planar γ-imaging and a SPECT/CT scan acquired in 4 healthy volunteers, the average effective whole-body dose estimation for administration of 700 MBq of ^{99m}Tc-PSMA I&S was 3.64 mSv, which is comparable to other ^{99m}Tc-based tracers.

IMPLICATIONS FOR PATIENT CARE: This study provides required data for translation and approval of ^{99m}Tc-PSMA I&S by regulatory agencies.

REFERENCES

1. Rajasekaran AK, Anilkumar G, Christiansen JJ. Is prostate-specific membrane antigen a multifunctional protein? *Am J Physiol Cell Physiol.* 2005;288:C975–C981.
2. Robu S, Schottelius M, Eiber M, et al. Preclinical evaluation and first patient application of ^{99m}Tc-PSMA-I&S for SPECT imaging and radioguided surgery in prostate cancer. *J Nucl Med.* 2017;58:235–242.
3. Horn T, Krönke M, Rauscher I, et al. Single lesion on prostate-specific membrane antigen-ligand positron emission tomography and low prostate-specific antigen are prognostic factors for a favorable biochemical response to prostate-specific membrane antigen-targeted radioguided surgery in recurrent prostate cancer. *Eur Urol.* 2019;76:517–523.
4. Maurer T, Robu S, Schottelius M, et al. 99MTechnetium-based prostate-specific membrane antigen-radioguided surgery in recurrent prostate cancer. *Eur Urol.* 2019;75:659–666.
5. Stabin MG, Sparks RB, Crowe E. OLINDA/EXM: the second-generation personal computer software for internal dose assessment in nuclear medicine. *J Nucl Med.* 2005;46:1023–1027.
6. International Commission on Radiological Protection (ICRP). The 2007 Recommendations of the International Commission on Radiological Protection. ICRP publication 103. *Ann ICRP.* 2007;37:259–293.
7. Eiber M, Herrmann K, Calais J, et al. Prostate Cancer Molecular Imaging Standardized Evaluation (PROMISE): proposed miTNM classification for the interpretation of PSMA-ligand PET/CT. *J Nucl Med.* 2018;59:469–478.
8. Ferrari M, De Marco P, Origgi D, et al. SPECT/CT radiation dosimetry. *Clin Transl Imaging.* 2014;2:557–569.
9. Santos-Cuevas C, Davanzo J, Ferro-Flores G, et al. ^{99m}Tc-labeled PSMA inhibitor: biokinetics and radiation dosimetry in healthy subjects and imaging of prostate cancer tumors in patients. *Nucl Med Biol.* 2017;52:1–6.
10. Hillier SM, Maresca KP, Lu G, et al. ^{99m}Tc-labeled small-molecule inhibitors of prostate-specific membrane antigen for molecular imaging of prostate cancer. *J Nucl Med.* 2013;54:1369–1376.
11. Vallabhajosula S, Nikolopoulou A, Babich JW, et al. ^{99m}Tc-labeled small-molecule inhibitors of prostate-specific membrane antigen: pharmacokinetics and biodistribution studies in healthy subjects and patients with metastatic prostate cancer. *J Nucl Med.* 2014;55:1791–1798.
12. Afshar-Oromieh A, Hetzheim H, Kübler W, et al. Radiation dosimetry of ^{68}Ga-PSMA-11 (HBED-CC) and preliminary evaluation of optimal imaging timing. *Eur J Nucl Med Mol Imaging.* 2016;43:1611–1620.
13. Giesel FL, Hadaschik B, Cardinale J, et al. F-18 labelled PSMA-1007: biodistribution, radiation dosimetry and histopathological validation of tumor lesions in prostate cancer patients. *Eur J Nucl Med Mol Imaging.* 2017;44:678–688.
14. Farolfi A, Gafita A, Calais J, et al. ^{68}Ga-PSMA-11 positron emission tomography detects residual prostate cancer after prostatectomy in a multicenter retrospective study. *J Urol.* 2019;202:1174–1181.
15. Matheoud R, Giorgione R, Valzano S, Sacchetti G, Colombo E, Brambilla M. Minimum acceptable sensitivity of intraoperative gamma probes used for sentinel lymph node detection in melanoma patients. *Phys Med.* 2014;30:822–826.